LONTAR KOMPUTER VOL. 14, NO. 3 DECEMBER 2023 **p-ISSN 2088-1541**
DOI : 10.24843/LKJITI.2023.v14.i03.p03 **e-ISSN 2541-5832**
Accredited Sinta 2 by RISTEKDIKTI Decree No. 158/E/KPT/2021

Enhanced Performance of Dynamic Neural Network Model using Wavelet Activation Functions

Syamsul Bahri[a,1], Lailia Awalushaumi[a,1], Nurul Fitriyani[b,3]

[a]Dept. of Mathematics, Faculty of Mathematics and Natural Sciences, University of Mataram
Jalan Majapahit No. 62 Mataram-NTB, Indonesia 83125
[b]Dept. of Statistics, Faculty of Mathematics and Natural Sciences, University of Mataram
Jalan Majapahit No. 62 Mataram-NTB, Indonesia 83125

[1]syamsul.math@unram.ac.id (Corresponding author)
[2]awalushaumi@unram.ac.id
[3]nurul.fitriyani@unram.ac.id

Abstract

Both static and dynamic adaptive neural networks have been broadly utilized in mathematical modeling and numerical analysis. This study aimed to enhance the accomplishment of Dynamic Neural Networks (DNN) models by applying wavelet functions as activation functions. Research that models and forecasts the intensity of solar radiation in Mataram City shows that combining B-Spline and Morlet wavelet activation functions can significantly increase the DNN model performance. Wavelet-DNN (W-DNN) was modeled with an identical architecture; the best showed the increase in the model achievement (0.7596 points for in-sample and 0.8502 points for out-sample data). Mainly for out-sample data, the model's performance using the W-DNN$^+$ intervention model increased by 4.0492 points.

Keywords: *Performance optimization of the model, adaptive neural networks, DNN Model, Wavelet, Solar Radiation.*

1. Introduction

Some aspects researchers consider as the basis for using the neural network model (NN) as an analytical tool include having adaptive abilities, learning algorithms by self, generalization abilities, and solving complex and complicated nonlinear problems [1]. Based on the time variable, the applications of the NN models can be divided into two categories, namely, static and dynamic neural network (SNN and DNN) models. The SNN model is based on a fixed time (static), while the DNN model develops according to changes in time (dynamic).

In terms of modeling solar radiation intensity, many studies have investigated the scatter scheme of the intensity of solar radiation in different locations using various methods and approaches. The other modeling techniques have been implemented by a combination method of empirical techniques and machine learning [2], deep learning model [3], six machine learning algorithms for daily global solar radiation and air temperature [4], multivariate time series based on NN method [5], ensemble artificial intelligence [6], and deep learning approach [7]. Meanwhile, those based on (static) neural network models include the ANN model with different learning algorithms [8], the modeling of solar radiation intensity in Mataram City, the hybrid wavelet-based model in Lombok Island, and SNN [9].

Introduced around 2000, the development and application of the DNN is a relatively new model after Warren McCulloch and Walter Pitts proposed the (static) neural network models in 1943 [10]. In its development, the DNN model has been applied to different research to address problems, including weather data forecasting [11], Zika virus risk forecasting [12], Time-varying inner wall temperature prediction [13], VGF crystal growth process forecast [14], diagnostic and detection fault [15], and wastewater effluent quality prediction [16].

The implementation of a DNN model using a recurrent neural network (Elman and Jordan) has been carried out by [11] to predict weather patterns, especially temperature, rainfall, and solar

radiation intensity in Anglesey (North Wales, UK). Similar research was carried out by [17] using meteorological data in the form of wind speed, wind direction, air humidity, air pressure, and rainfall to model and predict the intensity of solar radiation in Mataram City, West Nusa Tenggara using the DNN model to produce significant forecasts.

Combining two or more methods and models into one model to solve a problem is called a hybrid model. In practice, several studies show that the hybrid model shows significant results in terms of effectiveness and efficiency. In particular, research in [9] showed that the Wavelet Neural Network Model (static) could effectively model and estimate solar intensity. Furthermore, [17] has successfully modeled and predicted solar radiation intensity using the DNN model.

Based on the advantages of the hybrid model, this research combines the wavelet method and the neural network model to develop a hybrid model called Wavelet-DNN (W-DNN) using the neural network model as the core model and the wavelet method as a tool to optimize it. The W-DNN model is used to model and predict the intensity of solar radiation as a health indicator, especially in Mataram City.

2. Research Methods

2.1. Data and Data Organization

This study used the solar radiation data of Mataram City from June 2018 until May 2019, derived from the Environment and Forestry Agency, West Nusa Tenggara Province (Figure 1). Meteorological information was utilized, including wind speed, humidity, air temperature, air pressure, and rainfall as predictor data. Next, solar radiation data was used in response to predictor data.

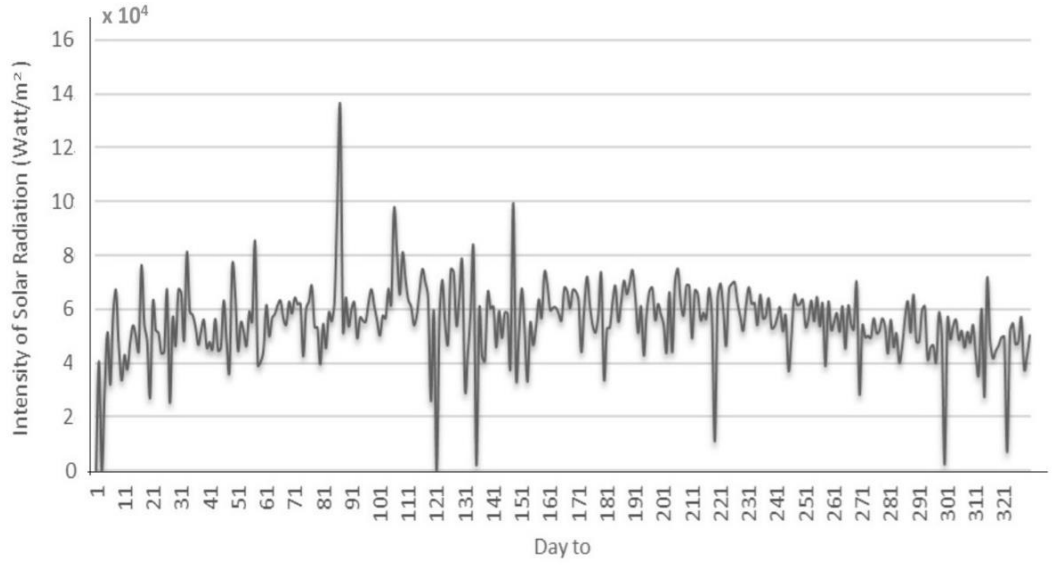

Figure 1. The intensity of solar radiation data of Mataram City from June 2018 until May 2019

Descriptively, the intensity of solar radiation data of Mataram City is given by several parameters, namely mean, max, min, and standard deviation of data, 55.3108, 135.3750, 0.00, and 14.2272, respectively.

Solar radiation intensity as an environmental parameter is affected by various meteorological specifics, including wind speed, air pressure, humidity, and rainfall. Solar radiation intensity can also be analyzed using time series data based on previous solar radiation intensities. Based on this situation, the intensity of solar radiation can be formulated as follows:

$$y(t) = f\left(x_1(t), x_2(t), x_3(t), x_4(t), x_5(t), y(t-k)\right), \quad \text{for some } k \in \mathbf{N}. \tag{1}$$

Variable $x_i(t),\ i=1,2,\cdots,5$ respectively denotes wind speed, humidity, air temperature, air pressure, and rainfall at time *t,* and variable *y* represents solar radiation's intensity.
The research data consisted of 325 data sets into two subsets, namely 280 (86.15%) training (in-sample) data and 45 (13.85%) testing (out-sample) data.

2.2. The Architecture of the Wavelet-Dynamic Neural Network (W-DNN) Model

The W-DNN architecture we propose consists of 6 layers: two initial layers, three hidden layers, and one output layer (Figure 2). The initial layer shows the data pre-processing process using the normalization method. The hidden layer depicts the data aggregation and activation process, and the output layer represents the hidden layer output aggregated into the model output. This W-DNN architecture was developed in our previous research [17].

2.3. Activation Function

This research model predicts solar radiation intensity as the impact of various meteorological and rainfall variables. The DNN Model uses the wavelet activation function, called the Wavelet-Dynamic Neural Network (W-DNN). The wavelet functions used are the B-spline Wavelet and the Morlet Wavelet.

The successful application of a neural network in data analysis depends on selecting the activation function used in the model. There were two types of wavelet functions used in this study, namely the B-Spline Wavelet [18] and the Morlet Wavelet, shown respectively by the following equations for any variable *x*:

$$\psi^n(x)=\frac{4b^{n+1}}{\sqrt{2\pi(n+1)\sigma_w^2}}\cos(2\pi f_0(2x-1))\exp\left(\frac{-(2x-1)^2}{2\sigma_w^2(n+1)}\right), \tag{2}$$

n denotes the order of the B-spline wavelet, a constant $b=0.657066,\ f_0=0.409177,$ and $\sigma_w^2=0.561145,$ and

$$\psi(x)=\exp(-x^2)\cos(5x) \tag{3}$$

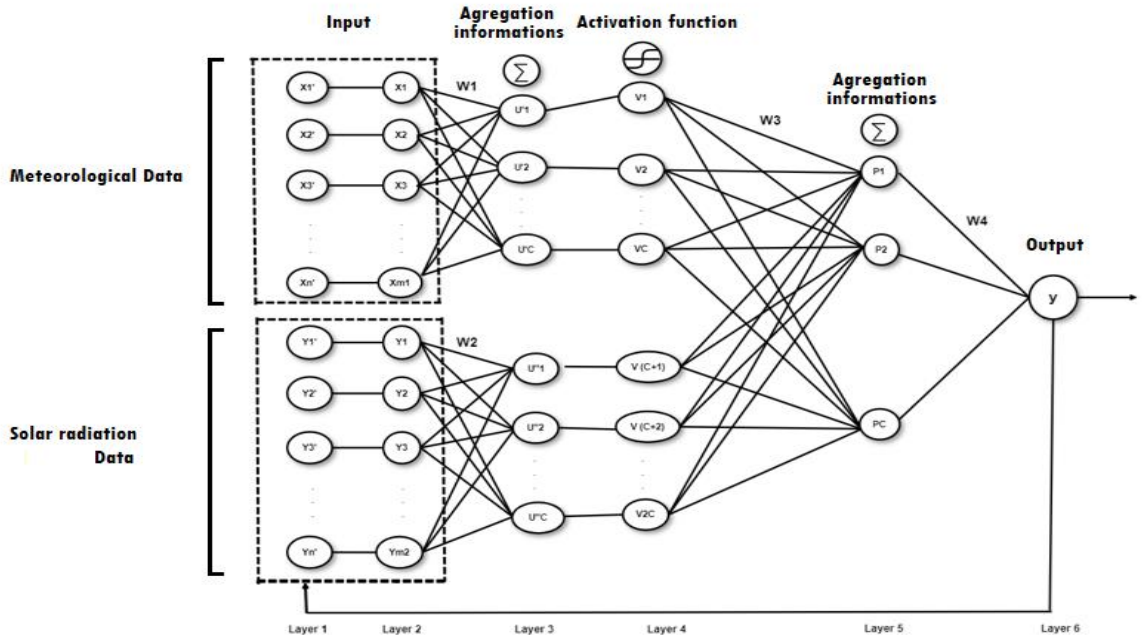

Figure 2. The proposed W-DNN architecture

2.4. Feed-Forward W-DNN procedures

The W-DNN feed-forward procedure offered in this research is basically on the architecture in Figure 2 and is provided through the following steps.

The 1st Layer: the input data is separated into two categories. The first input category, meteorological variables, including wind speed, temperature, humidity, air pressure, and rainfall, consists of m_1 data. The second input group comprises previous solar radiation data (lags) consisting of m_2 data.

The 2nd Layer: the input data was transformed through normalization methods by the following rules:

$$X_k = \frac{X'_k - X'_{\min}}{X'_{\max} - X'_{\min}} \tag{4}$$

where X'_k $X'_{\max}$, and $X'_{\min}$ correspondingly, indicate the *k -th, the minimum,* and the maximum values from the primary data set. The number of neurons was identical to the 1st Layer, namely $m = m_1 + m_2$ neuron.

The 3-rd Layer: If *C* is the number of classes of the input data, then each input data $X_k,\ k = 1,2,\cdots,m$ in the 2-nd Layer was aggregated by the rule:

$$U_j^1 = \sum_{i=1}^{m_1} W1_{ij} X_j;\ j = 1,2,\cdots,C \ \text{ dan } \ U_j^2 = \sum_{k=1}^{m_2} W1_{kj} X_j;\ j = 1,2,\cdots,C \tag{5}$$

where $W1_{ij}$ dan $W2_{kj}$ respectively represent weight matrices $m_1 \times C$ dan $m_2 \times C$, with $i = 1,2,\cdots,m_1$, $k = 1,2,\cdots,m_2$, dan $j = 1,2,\cdots,C$. The number of neurons in this Layer was 2*C* neuron.

The 4-th Layer: The weighted U_j^1 dan U_j^2 for $j = 1,2,\cdots,C$ was energized using wavelet functions, such as Wavelet B-Spline (Equation 2) and Wavelet Morlet (Equation 3).

The 5-th Layer: The activation result of U_j^1 dan U_j^2, let $V_j^1,\ j = 1,2,\cdots,C$ and $V_j^2,\ j = 1,2,\cdots,C$ was totaled again with weights $W_{31_{ij}}$ and $W_{32_{ij}}$, $i = 1,2,\cdots,C$ and $j = 1,2,\cdots,C$ using the equations as follows:

$$p_k^1(V_j^1) = \sum_{j=1}^{C} W_{31_{kj}} V_j^1,\ k = 1,2,\cdots,C. \tag{6a}$$

$$p_k^2(V_j^2) = \sum_{j=1}^{C} W_{32_{kj}} V_j^2,\ k = 1,2,\cdots,C. \tag{6b}$$

then

$$p_k(V_j) = \alpha_1 \times p_k^1(V_j^1) + \alpha_2 \times p_k^2(V_j^2),\ k, j = 1,2,\cdots,C \tag{6c}$$

for some constants α_1 and α_2.

The 6-th Layer: The terminal outputs of the W-DNN model are as the following:

Type a: $$y = \alpha \times \sum_{k=1}^{C} W4\, p_k + \beta,\ k = 1,2,\cdots,C \tag{7a}$$

Type b: $$y = \alpha \times \sum_{k=1}^{C} \mathrm{Max}\left(W4\right) p_k + \beta,\ k = 1,2,\cdots,C \tag{7b}$$

for fundamental constants *a* and *b*.

2.5. Learning Parameters Optimization

Optimizing the parameter was executed in the backward procedures of the W-DNN model. The optimized parameters contained weights $W1$, $W2$, $W31$, $W32$, and $W4$. Optimizing the parameter utilizing the momentum gradient descent, minimizing the cost function:

$$J = \frac{1}{N}\sum_{j=1}^{N}\left(y_j - y_j^d\right)^2 \tag{8}$$

N indicates the number of data, y_j and y_j^d correspondingly shows the output of the offered model and the *j*-th objective data, *j* = 1,2, …, N.

The optimizing procedure was accomplished using the partial differential formulas as follows:

$$\frac{\partial J}{\partial W_1} = \frac{\partial J}{\partial y}\frac{\partial y}{\partial p}\frac{\partial p}{\partial V^1}\frac{\partial V^1}{\partial U^1}\frac{\partial U^1}{\partial W_1} \tag{9}$$

$$\frac{\partial J}{\partial W_2} = \frac{\partial J}{\partial y}\frac{\partial y}{\partial p_2}\frac{\partial p_2}{\partial V^2}\frac{\partial V^2}{\partial U^2}\frac{\partial U^2}{\partial W_2} \tag{10}$$

$$\frac{\partial J}{\partial W_{31}} = \frac{\partial J}{\partial y}\frac{\partial y}{\partial p}\frac{\partial p}{\partial V^1}\frac{\partial V^1}{\partial W_{31}} \tag{11}$$

$$\frac{\partial J}{\partial W_{32}} = \frac{\partial J}{\partial y}\frac{\partial y}{\partial p}\frac{\partial p}{\partial V^2}\frac{\partial V^2}{\partial W_{32}} \tag{12}$$

$$\frac{\partial J}{\partial W4} = \frac{\partial J}{\partial y}\frac{\partial y}{\partial p}\frac{\partial p}{\partial W4} \tag{13}$$

Moreover, the procedure to improve weight used:

$$Wk_{ij} = Wk_{ij} + dW, \quad k = 1,2,3,4. \tag{14}$$

where,

$$dW = m \times Wk_{ij} - \eta_r \times (1-m) \times \partial Wk_{ij} \tag{15}$$

m, η_r, ∂Wk_{ij} with $k = 1,2,3,4$ correspondingly representing the momentum parameter, learning rate, and weight change $Wk,\ k = 1,2,3,4$ determined by Equations (9)-(13).

3. Results and Discussion

The Wavelet-Dynamics Neural Network (W-DNN) model proposed in this research is divided into two types: the Type-a Model, the W-DNN Model with output aggregation using weighted coefficients, and the Type-b Model, the W-DNN Model with output aggregation using the maximum coefficient.

3.1. W-DNN Models with Weighted Coefficients (Type-a)

Referring to equation (7a) and numerical simulation using the trial-and-error method, data modeling of solar radiation intensity that is influenced by meteorological data and rainfall using the DNN Wavelet Model with weighted coefficients is calculated by the following equations:

$$y = 1.035 \times \sum_{k=1}^{7} W4 \times p_k + 0.2492 \tag{16}$$

Where

$$p_k = 17.178 \times p_1(k,t) + 1.785 \times p_2(k,t)$$

Refer to Equations (5c), and $p_1(k,t)$ and the B-Spline Wavelet Equation (2), and $p_2(k,t)$ refer to the Morlet Wavelet Equation (3) give the result with an accuracy based on RMSE of 13.5306 with a graph as shown in Figure 3. Referring to equation (16) with the same indicator, namely RMSE, the model's accuracy on testing data (out-sample) is 17.6820.

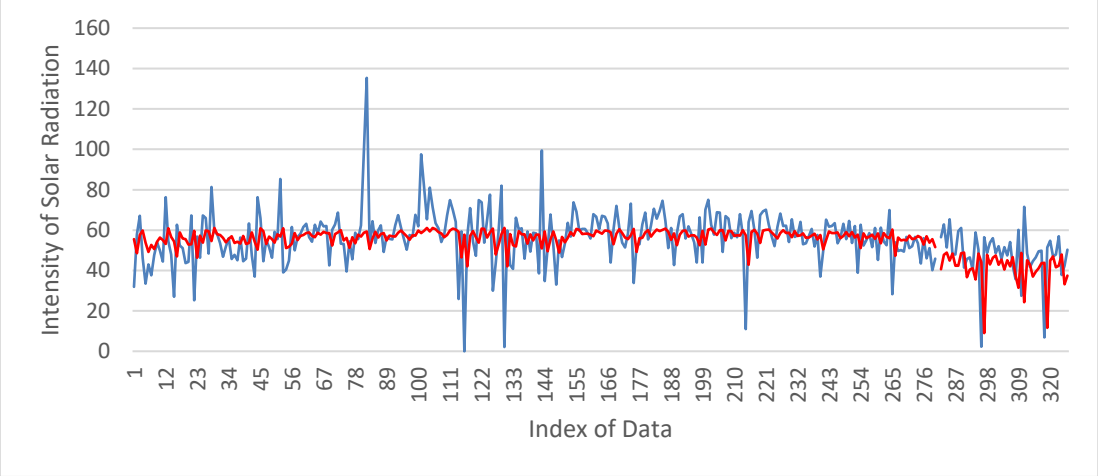

Figure 3. Comparison between actual data of solar radiation intensity (blue) and W-DNN model (red)

Descriptively, the W-DNN model implementation to the intensity of solar radiation data influenced by meteorological and rainfall data can be seen in Table 1. Based on Figure 3, it can be seen that the W-DNN model result curve tends to be close to the average and shows that the data pattern produced by the W-DNN model is generally similar to the characteristics of the actual data, especially in out-sample data. In this case, it can be seen that when the actual data graph increases or decreases, the model data also shows the same behavior. The statistics data in Table 1 reinforce that the average W-DNN model has a difference of 0.3663 points below the average actual data.

Table 1. The W-DNN model's performance on solar radiation intensity is determined by meteorological and rainfall variables.

Data	Statistical Indicator						Performa (RMSE)
	Min		Mean		Max		
	Model	Actual	Model	Actual	Model	Actual	
Training	42.0446	0	56.6543	57.0206	61.1037	135.3750	13.5306

Testing	10.9818	2.3077	47.7559	48.1202	56.4109	71.5429	17.6820
Testing+	14.8941	2.3077	47.1193	48.1202	54.6967	71.5429	16.3160

+ Intervention Model

By paying attention to the patterns formed, especially in the out-sample data, it can be seen that the model patterns are consistently below the actual data. If the constant factor can be viewed as an exogenous factor, and the addition of a constant value in equation (16) of 0.0850 points is a form of exogenous factor intervention, and other parameters are considered stable, then equation (16) given as below:

$$y = 1.035 \times \sum_{k=1}^{7} W4 \times p_k + 0.3342 \quad (17)$$

Applying equation (17) to the testing data (out sample) increases the model's performance for forecasting the intensity of solar radiation; initially, the RMSE was 17,680 to 16.3169. Graphically, the graph quality of testing data (out sample) is shown in Figure 4.

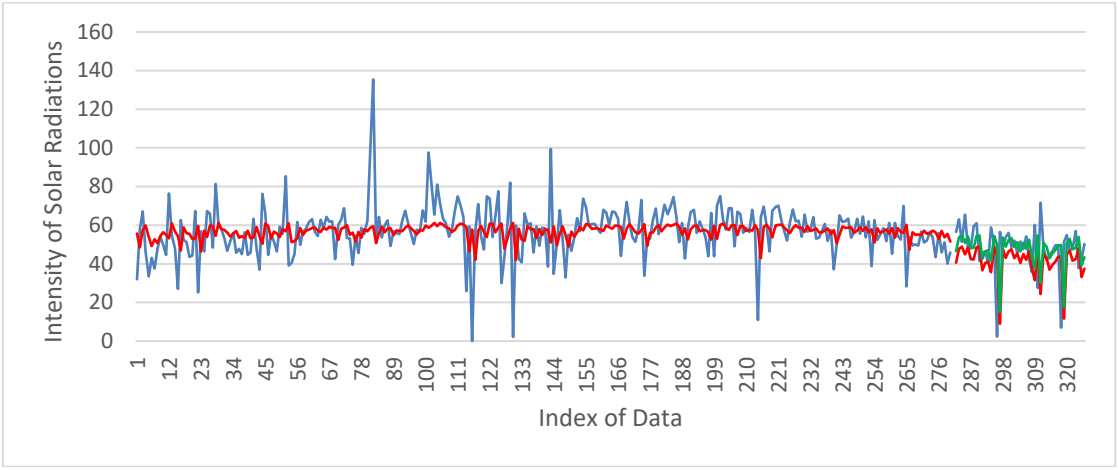

Figure 4. Graphical comparison between actual data of solar radiation intensity (blue) and W-DNN model (red) and improvement of W-DNN model curve on the testing data (green).

If observed specifically for the testing data, Figure 5 shows that the W-DNN Model given by equation (17), called the W-DNN+ Model, with a green graph, is more accurate than the original W-DNN Model with a red graph. This is statistically proven by the RMSE indicators of 16.3160 and 17.6820, respectively.

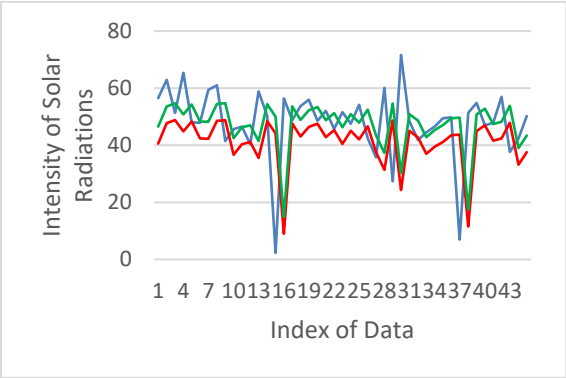

Figure 5. Graphic comparison of solar radiation intensity for testing data (out sample) between actual data (blue), W-DNN model data (red), and W-DNN+ intervention model (green)

3.2. W-DNN Model with Maximum Coefficient (Type-b)

Referring to equation (7b) and numerical simulation using the trial-and-error method, data modeling of solar radiation intensity that is influenced by meteorological data and rainfall uses the DNN Wavelet Model with the maximum coefficient given by the following equation:

$$y = 3.595 \times \sum_{k=1}^{7} Max\{W4\} \times p_k + 1.9999 \quad (18)$$

where

$$p_k = 0.8078 \times \ p_1(k,t) \ + \ 9.485 \ \times \ p_2(k,t)$$

Refer to equation (6c), and $p_1(k,t)$ refer to the B-Spline wavelet function in equation (2), and $p_2(k,t)$ refer to the Morlet wavelet function in equation (3), which gives results with RMSE-based accuracy of 13.5306 with a graph as shown in Figure 6. Referring to equation (18) with the same indicator, namely RMSE, the model accuracy for the testing data (out-sample) is obtained at 17.5422.

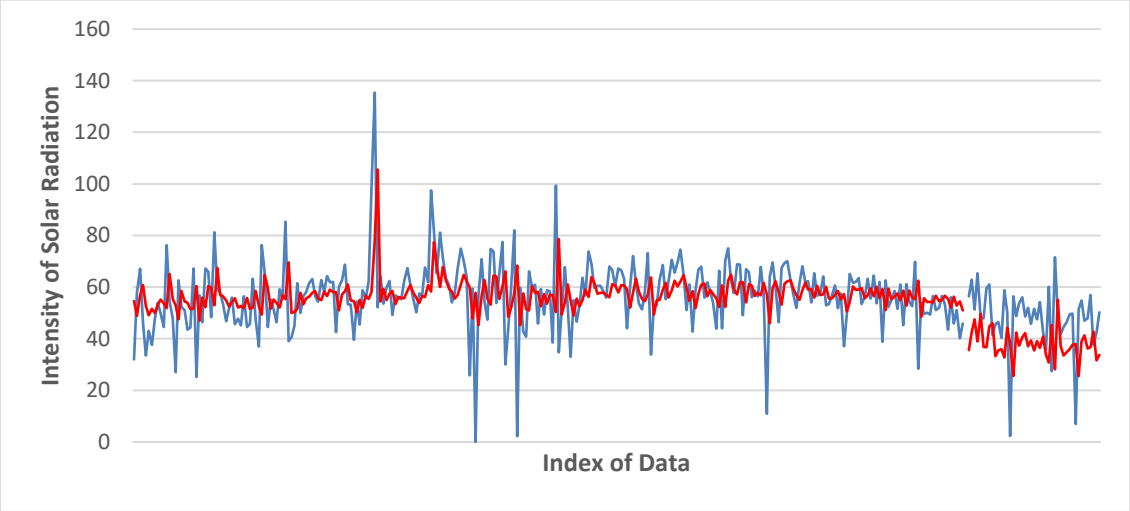

Figure 6. Graphical comparison of actual data on solar radiation intensity (blue) with the W-DNN model (red)

Descriptively, the application of the W-DNN model with maximum coefficients on solar radiation intensity data influenced by meteorological and rainfall data can be seen in Table 2. Figure 6 indicates that the yield curve of the W-DNN model with maximum coefficients tends to be close to the average and shows that the data pattern produced by the W-DNN model is generally similar to the characteristics of the actual data. In this case, it can be seen that when the actual data graph increases or decreases, the model data also shows the same behavior. This is reinforced by the statistical data in Table 2, which shows that the average W-DNN model has a difference of 0.0945 points above the average actual data.

Similar to the type-a model, paying attention to the patterns formed in the out-sample data shows that the model pattern is consistently below the actual data. If the constant factor is seen as an exogenous factor, and the addition of the constant value in equation (18) of 0.0850 points as a form of exogenous factor intervention, and other parameters are considered stable, equation (18) given as below:

$$y = 3.595 \times \sum_{k=1}^{7} Max\{W4\} \times p_k + 2.1491 \quad (19)$$

Applying equation (19) to the testing data (out sample) increases the model's performance for forecasting the intensity of solar radiation, from an RMSE of 17.5422 to 14.3432. The increase in graphical performance on the testing data (out sample) is shown in Figure 7.

Table 2. W-DNN model performance in modeling the intensity of solar radiation determined by meteorological and rainfall variables

Data	Statistical Indicator						Performa (RMSE)
	Min		Mean		Max		
	Model	Aktual	Model	Aktual	Model	Aktual	
Training	42.0446	0	57.1151	57.0206	105.5355	135.3750	13.9380
Testing	25.5104	2.3077	38.0180	48.1202	55.1116	71.5429	17.5422
Testing⁺	35.8403	2.3077	48.3479	48.1202	65.4415	71.5429	14.3432

⁺ Intervention Model

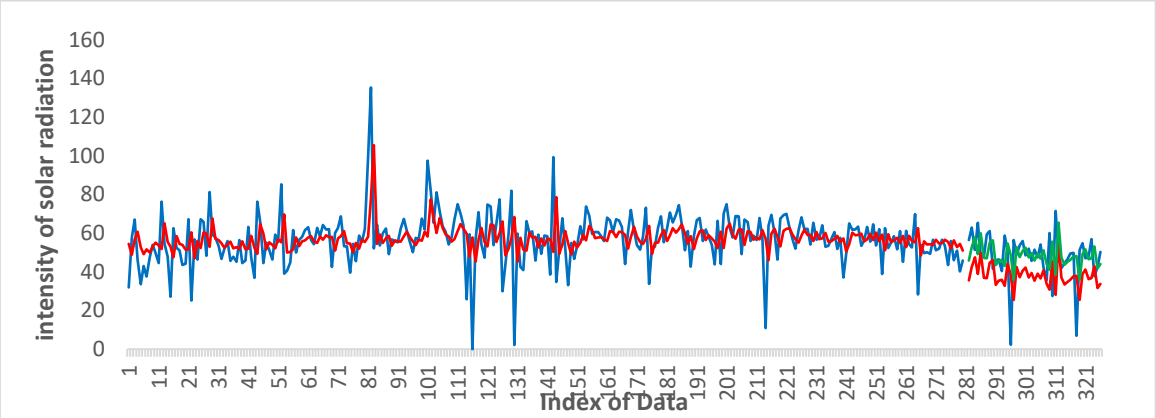

Figure 7. Graphical comparison of actual data between solar radiation intensity (blue) and the W-DNN model (red) and improvement of the W-DNN model curve on the testing data (green).

If observed specifically for the testing data, Figure 8 shows that the W-DNN Model given by equation (19), called the W-DNN⁺ model, with a green graph, is more accurate than the original W-DNN Model with a red graph. This is statistically proven by the RMSE indicators of 14.3432 and 17.5422, respectively.

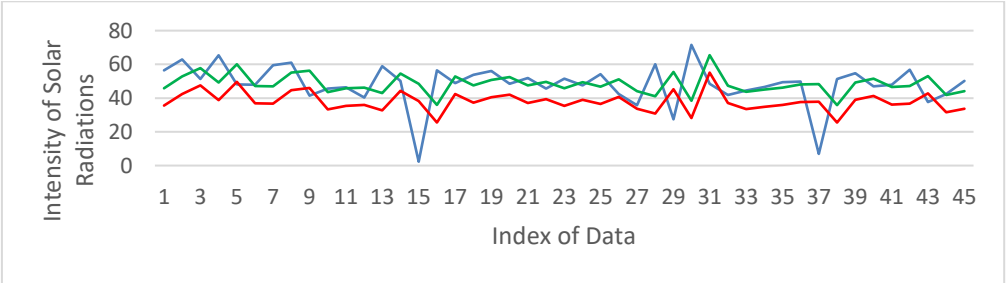

Figure 8. Graphical comparison of solar radiation intensity for testing data (out sample) between actual data (blue), W-DNN model data (red), and W-DNN⁺ intervention model (green)

Referring to the research conducted by [17], using the activation function from the wavelet function family improves the performance of the DNN model both for training data and testing

data (see Table 3). Performance comparison between the DNN and W-DNN models is shown in Table 3 below.

Table 3. Comparison of the DNN Model and the W-DNN Model

Model	Model Performance	
	In Sample Data	Out Sample Data
Type I-a DNN Model	14.2835	18.4005
Type I-b DNN Model	14.2802	18.7382
Type II-a DNN Model	14.5490	18.6353
Type II-b DNN Model	14.2802	18.3924
Type a W-DNN Model	13.5306	17.6820
Type a W-DNN^{+} Model		16.3160
Type b W-DNN Model	13.9380	17.5422
Type b W-DNN^{+} Model		14.3432

Remarks:
Type I-a DNN Model: binary sigmoid activation function and output aggregation process using weighted function.
Type I-b DNN Model: binary sigmoid type activation function and the output aggregation process using the maximum function.
Type II-a DNN Model: hyperbolic tangent type activation function and output aggregation process using weighted function.
Type II-b DNN Model: hyperbolic tangent type activation function and output aggregation process using maximum function.
Type-a Model W-DNN: the output aggregation process uses a weighted function.
Type-b Model W-DNN: aggregation process output using maximum function.
W-DNN^{+} Model: W-DNN model with an intervention coefficient

Based on Table 3, it can be seen that using the activation function from the wavelet function family can improve the performance of the DNN model, both for training data and testing data. For in-sample data, the W-DNN model with output values calculated using input aggregation using weighted coefficients tends to be better than the aggregation model using the maximum coefficient. As for the out-sample data, the W-DNN model with output values calculated using input aggregation using maximum coefficients tends to be better than the aggregation model using weighted coefficients. For training data, RMSE Model W-DNN Type A and Type B are 13.5306 and 13.9380, respectively. As for the testing data, RMSE Model Type A and Type B were 17.6820 and 17.5422, respectively. These results align with research conducted by [9] and [17].

The performance of the W-DNN Model, especially for testing data, can be improved by providing intervention to the W-DNN Model, both Type A and Type B, by adjusting the constant values in the model. For Type A, adding a constant value of 0.0850 points causes an increase in model performance of 1.366, from an RMSE of 17.6820 to 16.3160. Whereas for Type b, adding a constant value of 0.1492 points causes an increase in model performance of 3.199, from an RMSE of 17.5422 to 14.3432.

4. Conclusion

Case studies of modeling and forecasting the intensity of solar radiation as the effect of several meteorological and rainfall variables show that applying the wavelet function as an activation function in the Dynamic-Neural Network (DNN) Model can improve the models' performance. A performance increase occurs with both training and testing data. The W-DNN forecasting model performs better when constant parameters are adjusted as an exogenous factor.

5. Acknowledgments

The authors would like to thank the Chancellor of the University of Mataram for funding our research through the 2022 Research Capacity Building Program.

References

[1] S. Bahri, “Desain dan evaluasi performa model wavelet neural network untuk pemodelan,” *Ph.D. Dissertation, Gadjah Mada University Indonesia*, 2017.

[2] H. Zang, X. Jiang, L. L. Cheng, F. Zhang, Z. Wei, and G. Sun, "Combined empirical and machine learning modeling method for estimation of daily global solar radiation for general meteorological observation stations," *Renewable Energy*, vol. 195, 2022, doi: 10.1016/j.renene.2022.06.063.
[3] E. O. Yuzer and A. Bozkurt, "Deep learning model for regional solar radiation estimation using satellite images," *Ain Shams Engineering Journal*, 2022, doi: 10.1016/j.asej.2022.102057.
[4] M. K. Nematchoua, J. A. Orosa, and M. Afaifia, "Prediction of daily global solar radiation and air temperature using six machine learning algorithms; a case of 27 European countries," *Ecological Informatics*, vol. 69, 2022, doi: 10.1016/j.ecoinf.2022.101643.
[5] A. N. M. F. Faisal, A. Rahman, M. T. M. Habib, A. H. Siddique, M. Hasan, and M. M. Khan, "Neural networks based multivariate time series forecasting of solar radiation using meteorological data of different cities of Bangladesh," *Results in Engineering*, vol. 13, 2022, doi: 10.1016/j.rineng.2022.100365.
[6] F. Sohrabi Geshnigani, M. R. Golabi, R. Mirabbasi, and M. N. Tahroudi, "Daily solar radiation estimation in Belleville station, Illinois, using ensemble artificial intelligence approaches," *Engineering Applications of Artificial Intelligence*, vol. 120, 2023, doi: 10.1016/j.engappai.2023.105839.
[7] R. Gallo, M. Castangia, A. Macii, E. Macii, E. Patti, and A. Aliberti, "Solar radiation forecasting with deep learning techniques integrating geostationary satellite images," *Engineering Applications of Artificial Intelligence*, vol. 116, 2022, doi: 10.1016/j.engappai.2022.105493.
[8] A. Geetha *et al.*, "Prediction of hourly solar radiation in Tamil Nadu using ANN model with different learning algorithms," *Energy Reports*, vol. 8, 2022, doi: 10.1016/j.egyr.2021.11.190.
[9] S. Bahri, "Modeling of Solar Radiation Using the Wavelet Neural Network Model in Mataram City Lombok Island," *Lontar Komputer : Jurnal Ilmiah Teknologi Informasi*, vol. 11, no. 3, p. 178, Dec. 2020, doi: 10.24843/lkjiti.2020.v11.i03.p06.
[10] J. D. Rios, A. Y. Alanis, N. Arana-Daniel, C. Lopez-Franco, and E. N. Sanchez, *Neural networks modeling and control: Applications for unknown nonlinear delayed systems in discrete time*. 2020.
[11] A. J. Hussain, P. Liatsis, M. Khalaf, H. Tawfik, and H. Al-Asker, "A Dynamic Neural Network Architecture with Immunology Inspired Optimization for Weather Data Forecasting," *Big Data Research*, vol. 14, pp. 81–92, Dec. 2018, doi: 10.1016/j.bdr.2018.04.002.
[12] M. Akhtar, M. U. G. Kraemer, and L. M. Gardner, "A dynamic neural network model for predicting risk of Zika in real time," *BMC Medicine*, vol. 17, no. 1, Sep. 2019, doi: 10.1186/s12916-019-1389-3.
[13] X. Sun *et al.*, "Prediction of time-varying inner wall temperature of surge lines by a dynamic neural network," *Nuclear Engineering and Design*, vol. 383, 2021, doi: 10.1016/j.nucengdes.2021.111441.
[14] N. Dropka, M. Holena, S. Ecklebe, C. Frank-Rotsch, and J. Winkler, "Fast forecasting of VGF crystal growth process by dynamic neural networks," *Journal of Crystal Growth*, vol. 521, 2019, doi: 10.1016/j.jcrysgro.2019.05.022.
[15] G. Gravanis, I. Dragogias, K. Papakiriakos, C. Ziogou, and K. Diamantaras, "Fault detection and diagnosis for non-linear processes empowered by dynamic neural networks," *Computers & Chemical Engineering*, vol. 156, 2022, doi: 10.1016/j.compchemeng.2021.107531.
[16] Y. Yang *et al.*, "Prediction of effluent quality in a wastewater treatment plant by dynamic neural network modeling," *Process Safety and Environmental Protection*, vol. 158, 2022, doi: 10.1016/j.psep.2021.12.034.
[17] S. Bahri, M. R. Alfian, and N. Fitriyani, "Dynamic Neural Network Model Design for Solar Radiation Forecast," *Lontar Komputer : Jurnal Ilmiah Teknologi Informasi*, vol. 13, no. 2, p. 96, Aug. 2022, doi: 10.24843/LKJITI.2022.v13.i02.p03.
[18] M. Unser, "Ten Good Reasons for using Spline Wavelets," *Proceedings of SPIE – The International Society for Optical Engineering*, 1997.